Archives of Environmental Protection
Vol. 48 no. 4 pp. 25–34

PL ISSN 2083-4772
DOI 10.24425/aep.2022.143706

Comparative effectiveness of biochar derived from tropical feedstocks on the adsorption for ammonium, nitrate and phosphate

Ganghua Zou[1], Ying Shan[1], Minjie Dai[2], Xiaoping Xin[3], Muhammad Nawaz[4], Fengliang Zhao[1]*

[1]Environment and Plant Protection Institute, Chinese Academy of Tropical Agricultural Sciences, China
[2]Haikou Experimental Station, Chinese Academy of Tropical Agricultural Sciences, China
[3]University of Florida, United States
[4]Bahauddin Zakariya University, Pakistan

*Corresponding author's e-mail: zfl7409@163.com

Keywords: nutrients, soil amendment, adsorption model, biochars, tropical feedstock

Abstract: Biochar has been extensively studied as a soil amendment to reduce nutrients losses. However, the comparative effectiveness of biochar adsorption capacity for ammonium (NH_4-N), nitrate (NO_3-N), and phosphate (PO_4-P) remains unknown. In the present study, the effects of feedstock (banana stem and coconut shell) and temperature (300, 500, and 700°C) on biochar adsorption ability for NH_4-N, NO_3-N, and PO_4-P were investigated and fitted by three adsorption models, viz Freundlich, Langmuir, and linear. Freundlich (R^2 = 0.95–0.99) and Langmuir (R^2 = 0.91–0.95) models were found suitable for adsorption of NH_4-N. The maximum adsorption capacity (Q_m) for coconut shell biochar increased with pyrolysis temperature (Q_m = 12.8–15.5 mg g^{-1}) and decreased for banana stem biochar (Q_m = 12.9–9.7 mg g^{-1}). In the case of NO_3-N adsorption, Freundlich (R^2 = 0.82–0.99) and linear model (R^2 = 1.00) were found suitable while Langmuir model showed much less contribution, similarly adsorption of PO_4-P, was not supported by these three models. The minimum concentrations required for adsorption of phosphate were recorded as 36, 8, and 3 mg L^{-1} using pyrolyzed biochar at the temperatures of 300, 500, and 700°C, respectively. These results indicate that the feedstock and pyrolysis temperature, as well as aquatic nutrient concentration, were important factors for the adsorption of inorganic nitrogen and phosphorus.

Introduction

Nitrogen (N) and phosphorus (P) have been extensively used in agriculture for improving the crop growth and yield production to meet the demand of increasing population (Lu and Tian 2017). The consumption of N and P fertilizers in China in 2020 was up to 18.3 and 0.65 billion kg, respectively (Chinese statistical book report, 2021). Among these supplied nutrients from fertilizers, crops are unable to utilize all the nutrients and most of them are lost into the soil and environment, which can result in different environmental problems, like eutrophication and global warming (Carpenter et al. 2008, Tian et al. 2012). Thus, it is vital to improve the nutrient use efficiency for reducing their losses for agricultural sustainable development and environmental protection.

Currently, strategies such as organic fertilizers or straw returning, slow-release fertilizers and soil amendments have been used for increasing the nutrient use efficiency of fertilizers to cut down the applications rate of mineral fertilizers (Kim et al. 2017, Yin et al. 2018, Ye et al. 2020). Among the agronomic practices, the use of biochar is one of the useful approaches to improve the soil retention capacity and nutrient use efficiency. It has been reported that biochar amendments may enhance N uptake for rice and reduce the nutrient leaching in temperate soils (Laird et al. 2010, Huang et al. 2014). Biochar is a solid by-product synthesized through the pyrolysis of agricultural and forestry waste or even sewage sludge (Pulka et al. 2016, Piekarski et al. 2021). One of the best qualities of this synthesized biochar is that it consists of porous structure and has large specific surface area, which may be used for the adsorption of nutrients from soil solution or aqueous solution, as well as remediation of contaminated soil (Kong et al. 2014). The studies of many authors have reported the effects of biochar for the sorption of ammonium (NH_4-N), nitrate (NO_3-N), and phosphate (PO_4-P) from the soil or water solution (Hale et al. 2013, Gai et al. 2014). Zhou et al. (2019) used rice straw, sawdust, and egg shells for the biochar synthesis at the temperatures of 300, 500, and 700°C to examine the effects of phosphate and nitrate on the adsorption. They found that egg shells biochar was an effective way to remove PO_4-P and NO_3-N from wastewater, and its adsorption capacity (the amount of adsorbate taken up by the adsorbent per unit

mass of the adsorbent) increased with an increase in pyrolysis temperature. Hu et al. (2020) found that biochar synthesized at a low temperature (300°C) from the orange or pineapple peel had the strong NH_4-N adsorption capacities from water. There has been also a strong relationship between adsorbate concentration in aqueous solution and adsorption capacity of biochar, which can be estimated through different adsorption isotherm models (Fidel et al. 2018, Aghoghovwia et al. 2020). For ammonium, Fidel et al. (2018) found that the Langmuir and Freundlich models were good predictors for ammonium sorption isotherm. For nitrate adsorption, Aghoghovwia et al. (2020) conducted study on six biochars and found that they had a strong NO_3-N removal affinity from water, which was suitable with linear adsorption isotherm. Similar findings were also reported by Luo et al. (2019) about the nitrate removal from water by biochars derived from rice straw and swine manure to a great extent. For phosphate, Trazzi et al. (2016) showed that the adsorption of PO_4-P on sugar cane bagasse biochar increased with the increasing temperature (between 300 and 700°C) and fitted with both Freundlich and Langmuir models. Similarly, Zhao et al. (2017) also reported that pine biochar had a better phosphorus adsorption capacity than maize straw biochar and found that the adsorption curve was in line with Langmuir isotherm equation. However, several reports showed that biochar has no or very little ability to absorb nitrate and phosphate in soil (Yao et al. 2012). Hollister et al. (2013) found that no PO_4-P sorption from aqueous solution was observed using any corn stover biochar, and Luo et al. (2019) also reported that none of phosphate removals from water was achieved by all biochars derived from rice straw and swine manure. Additionally, the release of ammonium, nitrate and phosphate from biochars was observed.

Despite the growing interest in the application of biochar in agriculture to improve nutrient use efficiency, the comparative effectiveness of biochar synthesized by tropical feedstocks at different pyrolysis temperatures on the adsorption of ammonium, nitrate, and phosphate is rarely discussed, which are conducive to the application of biochar to reduce nutrient losses in tropical areas. Therefore, the objective of this study was to investigate

(i) impacts of tropical feedstock on the biochar adsorption of ammonium, nitrate, and phosphate;
(ii) effects of pyrolysis temperature for ammonium, nitrate, and phosphate adsorption;
(iii) evaluation of the relationship of adsorption isotherm with Freundlich, Langmuir model, and linear models;
(iv) determination of factors affecting the biochar adsorption for ammonium, nitrate, and phosphate.

Materials and Methods

Biochar preparation

Two typical tropical feedstocks comprising banana stem and coconut shells were collected in Hainan province of China to produce biochar at different pyrolysis temperatures. The feedstocks were firstly cut into pieces, dried in an oven, ground, and passed through the 0.25 mm mesh. The sieved feedstocks were put in a high-temperature furnace (KJ-A1200-121Z, China), and pyrolyzed under vacuum (-0.07 MPa) conditions for one hour at the temperatures of 300, 500, and 700°C, respectively. The rate of the temperature rise was 10°C per minute. The basic properties of feedstocks and biochar were determined. The infrared spectrums of biochar were measured by using FTIR spectrometer (Spectrum 100n, PerkinElmer, USA).

Adsorption experiment

About 0.2 g biochar was weighted and put in a 100 mL plastic centrifugal pipe having a lid, and the solutions of ammonium, nitrate, and phosphate (30 mL) were also added to the pipe and mixed. The ammonium chloride (Xilong Science Co., Ltd, China), potassium nitrate (Sinopharm Chemical Reagent Co., Ltd, China), and sodium phosphate (Xilong Science Co., Ltd, China) were used as the source for ammonium, nitrate, and phosphate solutions. The concentration gradients for ammonium and nitrate solutions were 15, 30, 60, 90, 120, 150, 180, 240, 300, 360, 420, and 480 mg N L^{-1} while the concentration gradients for phosphate solution were 0.2, 0.4, 0.8, 1.0, 1.5, 2.0, 3.0, 5.0, 8.0, 12.0, 15.0, 18.0, and 36 mg P L^{-1}. For each concentration, two repetitions were prepared. All the sample solutions were shaken for 24 h at 25°C with a speed of 200 rpm and then filtered. The filtrates of the solutions were used to determine the corresponding concentrations of inorganic nitrogen and phosphate.

The measurement for properties

For each property, two repetitions of samples were prepared to measure. The yield rate of biochar was calculated as the ratio of derived biochar mass to raw material mass. The pH of biochar was determined by pH meter (PHS-3C, INESA, China) with the 1:40 ratio of biochar and water. The contents of biochar carbon (C), hydrogen (H), nitrogen (N), and sulfur (S) were determined by element analyzer (EA2400-II, PerkinElmer, USA). The electrical conductivity (EC) of biochar was measured by conductivity meter (DDS-307, INESA, China) with the 1:40 ratio of biochar and water. 3.5 g biochar was mixed with 50 mL 1.66 cmol L^{-1} hexamine cobalt trichloride ($Co(NH_3)_6Cl_3$) solution and then shaken horizontally for one hour at 25°C at a speed of 200 rpm. The filtrate was analyzed by ultraviolet visible spectrophotometer (DR 6000, HACH, USA) to determine cation exchange capacity (CEC) following the method of Ciesielski and Sterckeman (1997). The BET specific surface area of biochar was measured by specific surface analyzer (ASAP 2460, Micromeritics, USA). The biochar ash content was measured by the ratio of left biochar mass to the initial mass after burning at 550°C for one hour. Biochar was digested completely by H_2SO_4 and H_2O_2 using electric furnace (SN-DL-1, sunne, China) and the digestion solution was used for the determination of total phosphorus content using a molybdenum antimony anti-colorimetric method (Bao 2000), while the total potassium contents were measured using flame photometer (M410, Sherwood, England). The filtrate was also used to measure total calcium and magnesium contents by atomic absorption spectrophotometer (PinAAcle 900T, PerkinElmer, USA). After obtaining the adsorption equilibrium, the solution was filtered and the filtrate was used for the determination of ammonium, nitrate and phosphate concentrations by using the indophenol blue colorimetry method (Bao 2000), the dual wavelength spectrophotometry method (Norman et al. 1985) and the molybdenum antimony anti-colorimetric method (Bao 2000).

Formation of adsorption models for ammonium, nitrate, and phosphate

For the development of models, the equilibrium concentration (Q_e) was:

$$Q_e = \frac{(C_0 - C_e) \cdot v}{m}$$

The linear isotherm model:

$$Q_e = a \cdot C_e + b$$

The Freundlich model (Freundlich 1907):

$$\ln Q_e = lnK_F + \frac{1}{n} \cdot lnC_e$$

The Langmuir model (Langmuir 1916):

$$\frac{C_e}{Q_e} = \frac{1}{Q_m \cdot K_L} + \frac{1}{Q_m} \cdot C_e$$

Where: Q_e is the amount of N or P retained by biochar (mg g^{-1}) at equilibrium; C_0 are C_e the concentrations of N or P in the initial and equilibrium solution (mg L^{-1}), respectively; v is the volume of aqueous solution (L); m is biochar mass (g). The a, b, K_F (L g^{-1}) and K_L (L mg^{-1}) are the empirical constants of model; $\frac{1}{n}$ is the measure of intensity. K_F refers to the partition coefficient between solution and biochar. Q_m is the maximum adsorption capacity of biochar (mg g^{-1}). When $n = 1$, the Freundlich model will reduce to the linear model.

Data analysis

All the obtained data were organized with Microsoft Excel 2017. The model fitting processes for the biochar adsorption of ammonium, nitrate, and phosphate were also carried out in Excel software. The infrared spectrum of biochar was plotted in Excel software using the data of wave number and absorbance produced by FTIR spectrometer.

Results

Effect of pyrolysis temperatures on biochar properties

Biochar synthesized from both banana stem and coconut shell feedstocks showed the rapid response with the change of pyrolysis temperatures. The content of hydrogen, nitrogen, and sulfur and yield rate decreased with the increasing pyrolysis temperatures (Table 1). The NO_3-N, NH_4-N, and PO_4-P concentrations of biochar were also decreased with the increase of temperatures. However, the ratio of carbon to nitrogen (C/N), total phosphorus (P), total potassium (K), ash content, pH, and EC increased with the increase of pyrolysis temperatures. There were great differences in carbon (C), total calcium (Ca), total magnesium (Mg), cation exchange capacity (CEC), and specific surface areas (SSA) were noted in biochar derived from banana stem and coconut shell. As for coconut shell biochar, the highest C content and CEC were found at 500°C, while less amount was observed at 700°C. The Ca and Mg contents were also found higher at 500°C and lower at 300°C, while SSA of biochar increased with the rise of temperatures. However, in banana stem biochar, the C content increased with the increase of temperatures, but the CEC and Mg contents decreased with the increasing temperatures. The Ca and SSA of biochar derived from banana feedstock were also found higher at 500°C. The K content and EC were found higher in banana stem biochar as compared to coconut shell biochar (Table 1).

For all the biochars synthesized at different temperatures, the main functional groups were hydroxyl group (O-H)

Table 1. The properties of feedstocks and biochars

Properties	CS	CS300	CS500	CS700	BS	BS300	BS500	BS700
Carbon (%)	47.6	66.2	69.1	61.1	38.6	47.4	48.2	49.2
Hydrogen (%)	5.50	4.21	3.18	1.88	5.15	4.18	2.51	1.60
Nitrogen (%)	0.69	0.92	0.88	0.48	0.58	1.07	0.92	0.73
Sulfur (%)	0.97	0.82	0.48	0.31	0.94	0.74	0.37	0.18
C/N ratio	69	72	79	127	67	44	52	67
Total phosphorus (g kg^{-1})	0.85	1.82	3.35	3.07	1.32	3.63	4.59	4.39
Total potassium (g kg^{-1})	12.0	24.3	30.1	34.8	73.4	126.0	167.1	198.0
Total calcium (g kg^{-1})	0.83	9.22	11.6	11.0	7.08	18.1	25.2	21.5
Total magnesium (g kg^{-1})	0.80	1.87	3.56	2.70	1.75	5.14	4.89	4.46
Ash content (%)	3.26	9.28	12.9	20.2	14.9	24.6	36.6	37.9
Yield rate (%)	–	50.4	40.6	34.6	–	55.5	39.8	37.6
pH	–	8.2	9.3	9.6	–	8.0	10.0	10.2
EC (μS cm^{-1})	–	398	525	720	–	3175	4244	4455
CEC (cmol kg^{-1})	–	30.4	53.3	25.9	–	63.6	62.5	58.0
SSA (m^2 g^{-1})	–	3.20	5.40	82.8	–	2.60	3.10	2.20
NO_3-N (mg kg^{-1})	–	174.6	94.0	88.9	–	73.4	44.4	38.8
NH_4-N (mg kg^{-1})	–	511.2	31.0	30.1	–	132.8	145.6	36.4
PO_4-P (mg kg^{-1})	–	1353.9	347.7	310.7	–	1037.5	297.5	394.4

Note: EC refers to electrical conductivity; C/N ratio refers to the ratio of carbon content to nitrogen content. CEC was cation exchange capacity; SSA denotes specific surface area; NO_3-N, NH_4-N, and PO_4-P refer to nitrate nitrogen, ammonium nitrogen, and phosphate content, respectively. CS and BS denote coconut shell and banana stem raw material, respectively; CS300, CS500, and CS700 denote coconut shell biochar derived in 300, 500, and 700°C, respectively; BS300, BS500 and BS700 denote banana stem biochar derived in 300, 500, and 700°C, respectively

(3600–3440 cm^{-1}) and aromatic (C=C) or carbonyl group (C=O) (1640–1623 cm^{-1}). As shown in Figure 1a, the hydroxyl group content of coconut shell biochar increased with the increasing pyrolysis temperature and the change of hydroxyl group content between 700°C and 500°C was less than that between 500°C and 300°C. Similarly, aromatic group content was also found higher at 500°C, and much lower at 300°C. It was also observed that aromatic group content increased faster from 300°C to 500°C, while it was a little slower from 500°C to 700°C. As for banana stem biochar, the hydroxyl group content increased with the increasing pyrolysis temperature but the change between 700°C and 500°C was also found faster than that between 500°C and 300°C (Figure 1b). The aromatic group content of biochar produced at 700°C was also observed higher.

Adsorption of ammonium on biochar

The adsorption capacity varied with the feedstock types and pyrolysis temperatures. Both Freundlich and Langmuir isothermal adsorption models could describe the adsorption of ammonium by coconut shell biochar and banana stem biochar. It needs to be mentioned that a higher correlation coefficient (R^2 = 0.95–0.99) was observed in Freundlich as compared to Langmuir model (R^2 = 0.91–0.95) (Figure 2). Moreover, the maximum adsorption capacity (Q_m) for coconut shell biochar increased with the increase of pyrolysis temperature and decreased for the banana stem biochar. Coconut shell biochar at 700°C showed the higher sorption capacity (Q_m = 14.5 mg g^{-1}) compared to the banana stem biochar that was recorded lower (Q_m = 9.7 mg g^{-1}) at the same temperature (Table 2). These findings suggest that both feedstock and pyrolysis temperature affected the capability of biochar for the adsorption of ammonium in solutions.

Adsorption of nitrate on biochar

The adsorption of nitrate by biochar was observed effectively in solutions. Three models were found fit for the adsorption of nitrate by biochar derived from coconut shell and banana stem

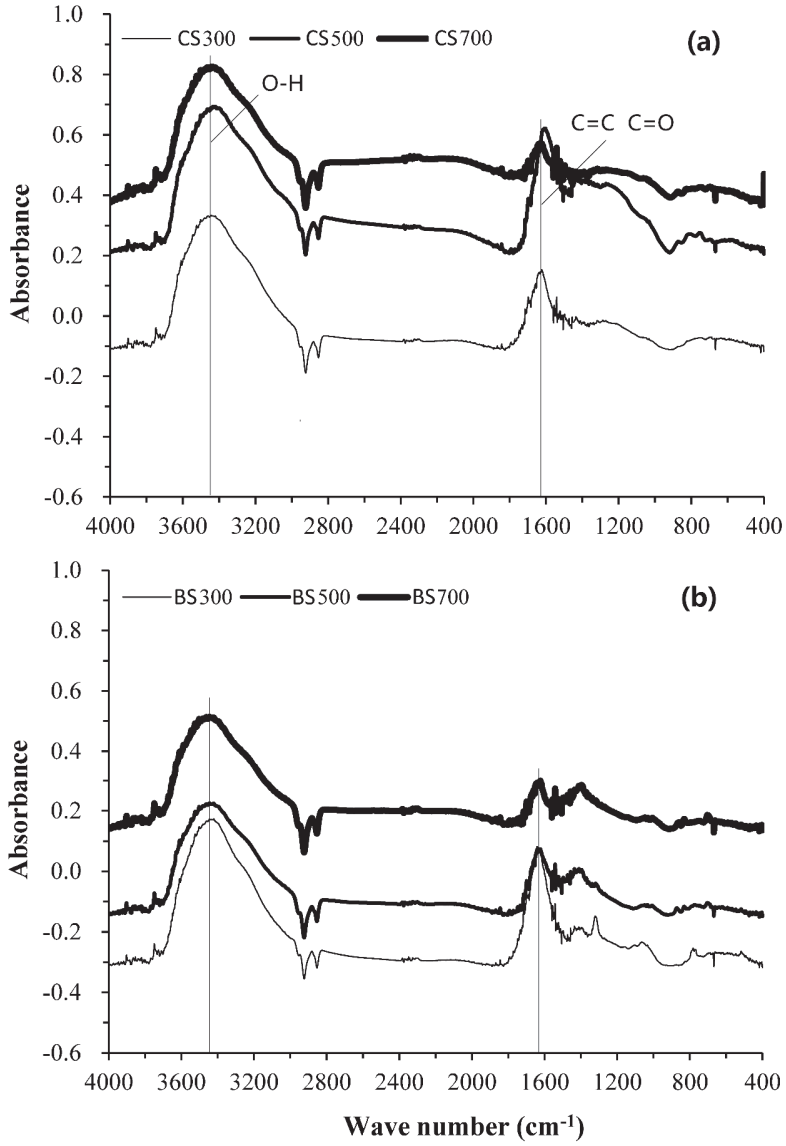

Fig. 1. The infrared spectra of biochar at different pyrolysis temperatures. CS300, CS500 and CS700 denote coconut shell biochar derived at 300, 500 and 700°C, respectively; BS300, BS500 and BS700 denote banana stem biochar derived at 300, 500, and 700°C, respectively

(Figure 3). Based on the R^2 as described in Table 3, Freundlich model and linear model were found more useful than Langmuir model for both feedstocks. Among all models, the efficiency of the linear model was found more suitable as compared to that of the other two ones. During the adsorption process of nitrates by biochar, it was observed that the adsorption rate of nitrates by biochar enhanced with the increasing concentration of NO_3-N.

Adsorption of phosphate on biochar

As showed in Table 4, both Freundlich model and Langmuir model did not fit the biochar adsorption for phosphate, which was affected by the feedstock, pyrolysis temperature, and phosphate concentration. As the phosphate concentration in solutions (C_0) increased up to 36 mg L^{-1}, all coconut shell biochar prepared at different temperatures did not adsorb phosphate, but released phosphate from biochar itself into the solutions (Figure 4). The adsorption of biochar on phosphate was influenced by pyrolysis temperature and phosphate concentration as indicated that only biochar prepared at 300°C absorbed the phosphate when the concentration of phosphate raised up to 36 mg L^{-1}. The adsorption of biochar produced at 500°C for phosphate started when the phosphate concentration in solutions was higher than 8 mg L^{-1}, while the adsorption of biochar produced at 700°C started in the solutions with the phosphate concentration of 3 mg L^{-1}. Therefore, the minimum phosphate concentration for biochar adsorption decreased with the increasing pyrolysis temperature. When the concentration

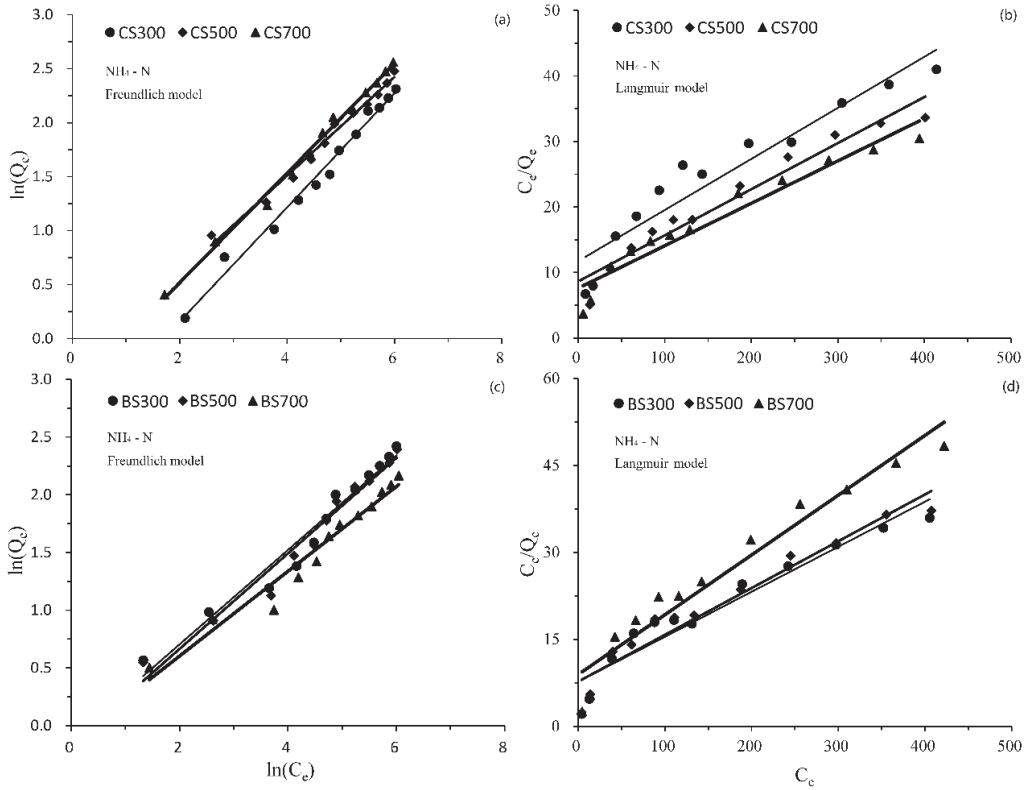

Fig. 2. The model fitting of ammonium nitrogen adsorption by biochar. CS300, CS500 and CS700 denote coconut shell biochar derived at 300, 500, and 700°C, respectively; BS300, BS500 and BS700 denote banana stem biochar derived at 300, 500 and 700°C, respectively. Q_e (mg g^{-1}) and C_e (mg L^{-1}) are the amount of adsorbed ammonium nitrogen and ammonium nitrogen concentration in the solution at equilibrium, respectively. NH_4-N refers to ammonium nitrogen

Table 2. The model parameters for ammonium nitrogen adsorption by biochar

Feedstock	T(°C)	Freundlich model			Langmuir model		
		R^2	n	K_F	R^2	Q_m	K_L
CS	300	0.99	1.89	0.41	0.91	12.8	0.007
	500	0.95	2.19	0.73	0.95	14.2	0.008
	700	0.99	1.97	0.61	0.94	15.5	0.008
BS	300	0.96	2.45	0.89	0.93	12.9	0.010
	500	0.97	2.42	0.85	0.94	12.4	0.010
	700	0.96	2.72	0.88	0.94	9.7	0.012

Note: R^2 is the determination coefficient of model; n, K_F (L g^{-1}) and K_L (L mg^{-1}) are empirical constants of model; Q_m is the maximum adsorption capacity of biochar (mg g^{-1}). CS and BS refer to coconut shell and banana stem raw material, respectively. T denotes pyrolysis temperature of biochar production

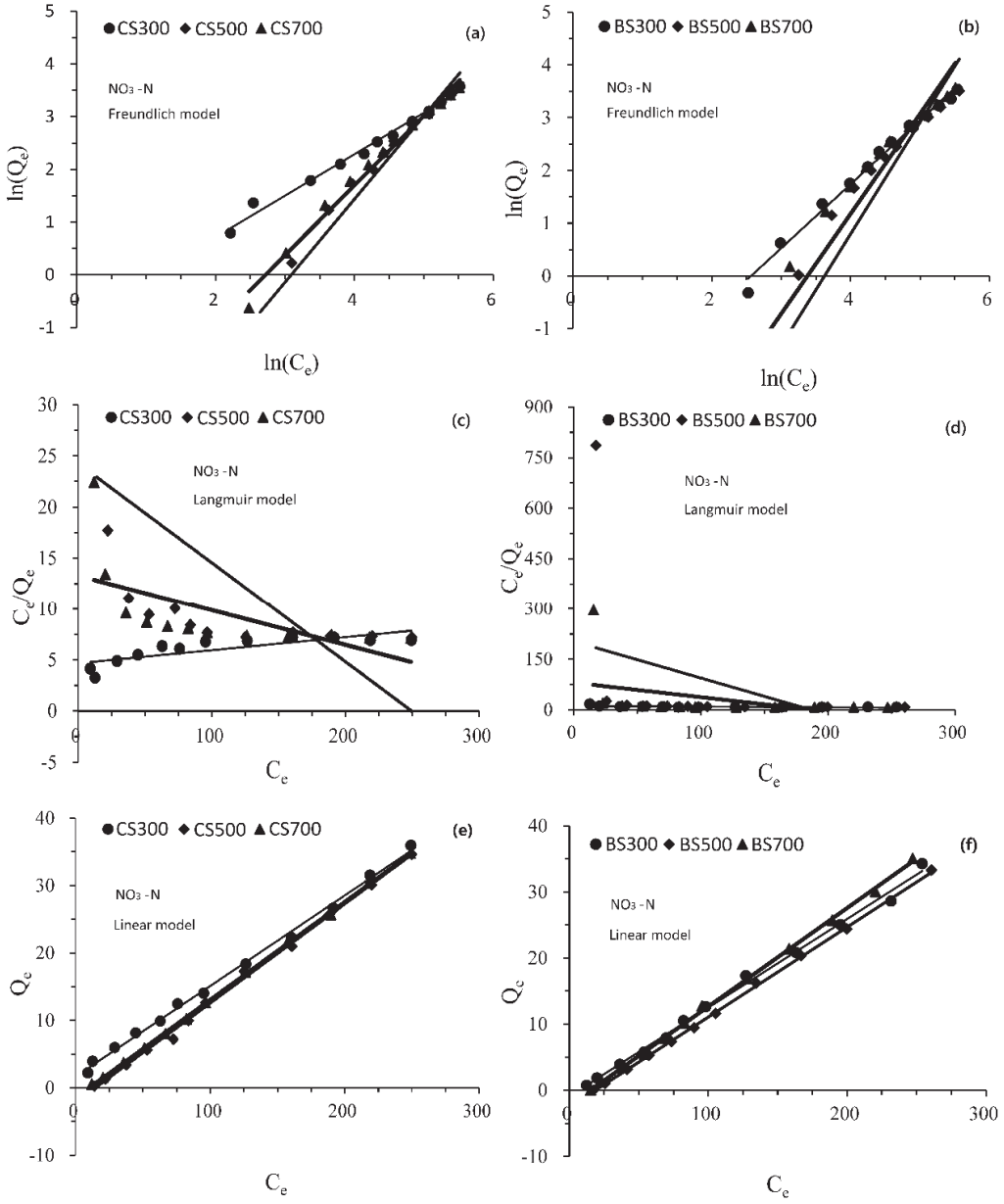

Fig. 3. The model fitting of nitrate nitrogen adsorption by biochar. CS300, CS500 and CS700 denote coconut shell biochar derived at 300, 500 and 700°C, respectively; BS300, BS500 and BS700 denote banana stem biochar derived at 300, 500 and 700°C, respectively. Q_e (mg g^{-1}) and C_e (mg L^{-1}) are the amount of adsorbed ammonium nitrogen and ammonium nitrogen concentration in the solution at equilibrium, respectively. NO_3-N refers to nitrate nitrogen

Table 3. The model parameters for nitrate nitrogen adsorption by biochar

Feedstock	T(°C)	Freundlich model			Langmuir model			Linear model	
		R^2	n	K_F	R^2	Q_m	K_L	R^2	*Equation*
CS	300	0.99	1.27	0.426	0.65	78.1	0.003	1.00	Q_e=0.134*C_e+1.657
	500	0.95	0.63	0.008	0.25	-10.3	-0.004	1.00	Q_e=0.147*C_e-2.154
	700	0.99	0.76	0.028	0.37	-29.4	-0.003	1.00	Q_e=0.145*C_e-1.477
BS	300	0.99	0.82	0.045	0.16	-0.92	-0.005	1.00	Q_e=0.134*C_e-0.906
	500	0.82	0.47	0.000	0.16	-2.34	-0.005	1.00	Q_e=0.136*C_e-2.534
	700	0.86	0.53	0.002	0.35	-50.5	-0.002	1.00	Q_e=0.149*C_e-2.235

Note: R^2 is the determination coefficient of model; n, K_F (L g^{-1}) and K_L (L mg^{-1}) are empirical constants of model; Q_m is the maximum adsorption capacity of biochar (mg g^{-1}). CS and BS refer to coconut shell and banana stem raw material, respectively. T denotes pyrolysis temperature for biochar production. Q_e (mg g^{-1}) and C_e (mg L^{-1}) are the amount of adsorbed N or P, and the N or P concentration in the solution at equilibrium, respectively

was less than 3 mg L^{-1}, the banana stem biochar did not adsorb phosphate from solutions, but released it into the solutions from biochar itself.

Discussion

The adsorption of ammonium by biochar

For ammonium, all the biochar in the present study adsorbed ammonium from aqueous solutions, which agreed with the previous studies (Gai et al. 2014, Hou et al. 2016, Luo et al. 2019), and the adsorption were found to be well fitted by Freundlich and Langmuir models. Many studies reported that the possible adsorption mechanisms of ammonium on biochar include surface complexion, cation exchange capacity, and electrostatic attraction (Jassal et al. 2015, Hou et al. 2016, Fiderl et al. 2018, Hu et al. 2020). Besides, it has also been reported that most of the ammonium sorption may be due to physical entrapment of NH_4-N in biochar pores, and well fitted by Freundlich and Langmuir models (Wang et al. 2015). However, the maximum adsorption capacities (Q_m) of biochar derived from the two feedstocks varied. The biochar derived from coconut shell at 700°C showed the most Q_m and the least at 300°C. The opposite result was observed for banana stem biochar. Previously, Yin et al. (2018) highlighted the highest NH_4-N adsorption capacity by sesame straw biochar prepared at 300°C due to its abundant surface functional groups. Similar findings have also been found by Hu et al. (2020) and Xu et al. (2019) who reported that biochars produced at low temperatures showed better NH_4-N adsorption capacity. The reason might be due to the different specific surface area (SSA). Coconut shell biochar had more SSA at the pyrolysis temperature of 700°C, but banana stem biochar showed less SSA at higher temperature (Table 1). However, Xu et al. (2019) hypothesized that zeta potential and C/H ratio, rather than surface area, were the most important factors in determining biochar sorption potential for NH_4-N. Takaya et al. (2016) also suggested that the surface area was not the most important factor influencing biochar ammonium adsorption capacity, and suggested that NH_4-N adsorption may have occurred mainly via chemical reactions with oxygen-containing functional groups rather than ion-exchange/physisorption. Therefore, there is dire need to study these differences for better understanding of the trend of

Table 4. The model parameters for phosphorus adsorption by biochar

Feedstock	T(°C)	Freundlich model			Langmuir model		
		R^2	n	K_F	R^2	Q_m	K_L
CS	300	0.19	17.3	0.630	0.95	0.86	0.617
	500	0.48	1.01	0.009	0.01	-0.35	-0.014
	700	0.63	0.98	0.006	0.02	-0.34	-0.013
BS	300	0.59	0.50	0.002	0.11	-0.28	-0.032
	500	0.97	0.73	0.035	0.53	-2.47	-0.023
	700	0.72	0.76	0.088	0.16	-2.77	-0.036

Note: R^2 is coefficient of determination; n, K_F (L g^{-1}) and K_L (L mg^{-1}) are empirical constants of model; Q_m is the maximum adsorption capacity of biochar (mg g^{-1}). CS and BS refer to coconut shell and banana stem raw material, respectively. T denotes pyrolysis temperature for biochar production

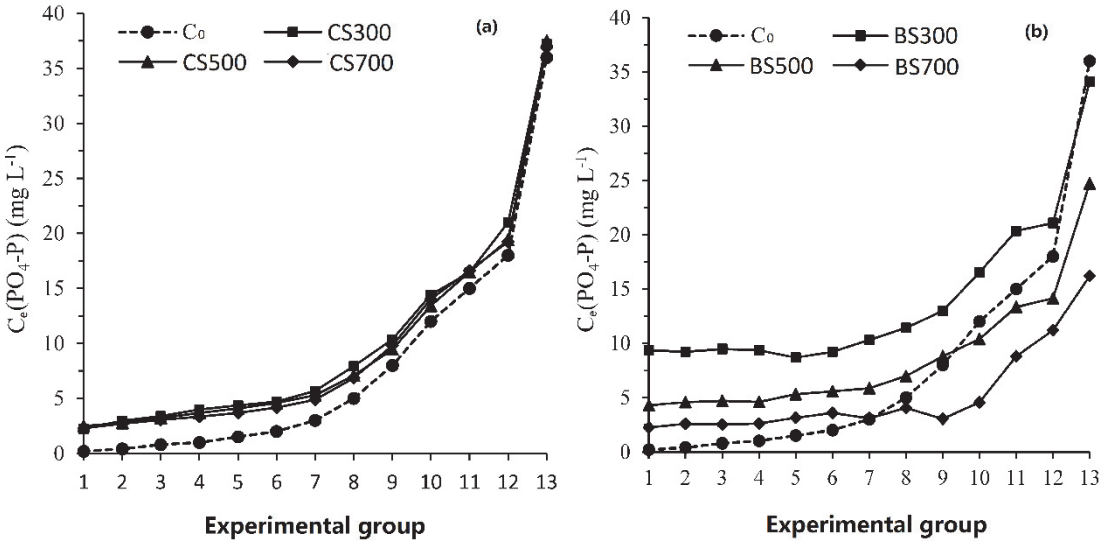

Fig. 4. The comparison of phosphate concentration in water between equilibrium state and initial state with different biochars. CS300, CS500, and CS700 denote coconut shell biochar derived at 300, 500, and 700°C, respectively; BS300, BS500, and BS700 denote banana stem biochar derived at 300, 500, and 700°C, respectively. The C_e and C_0 refers to the equilibrium and initial phosphate concentration of aqueous solution, respectively.

biochar adsorption capacity for ionic adsorption. Perhaps the major factors for ammonium adsorption on different biochars might not be completely consistent.

The adsorption of nitrate by biochar

The present study found that biochar adsorption for nitrate was affected by nitrate concentrations. Banana stem biochar produced at all the three-pyrolysis temperatures adsorbed nitrate in solutions when nitrate concentration was up to 30 mg L^{-1}, but only 15 mg L^{-1} for coconut shell biochars. In the previous studies, there were two opposite conclusions for nitrate adsorption on biochar. It was noticed that nitrate sorption was not effective for corn stover biochar and oak wood biochar derived from different pyrolysis temperatures, as well as for wheat-straw biochar and peanut-shell biochar. Instead, some nitrate was even released from the biochar materials (Hollister et al. 2013; Gai et al. 2014). Zhou et al. (2019) also reported that the biochar prepared from the plant wastes had the limited adsorption or even released nitrate, but egg shell biochar absorbed much nitrate and its adsorption capacity increased with the increasing pyrolysis temperatures. However, Zhao et al. (2018) found that corn cob biochar produced at 600°C was a better nitrate adsorbent than peanut shell biochar and cotton stalks biochar. Kameyama et al. (2016) indicated that biochar produced at 800°C had the greatest NO_3-N adsorption. Biochar produced at higher temperature adsorbed much nitrate because of having good thermal stability, porous structure, abundant surface functional groups, and higher surface area (Zhao et al. 2018). Vijayaraghavan and Balasubramanian (2021) suggested that pinewood waste biochar prepared at 600°C showed the maximum uptake for nitrate because of high C content, pore volume, and surface area. In the present study, relatively less difference was observed for both biochars derived from coconut shell and banana stem at different pyrolysis temperatures for the nitrate adsorption. The reason may be that the initial nitrate concentration in biochar, CEC, carbon content, and SSA of biochar should be taken into account comprehensively. Because we found that although the CEC and carbon content of coconut shell biochar at 500°C were higher, their SSA was the lowest, while when the carbon content of banana stem biochar at 700°C was high, its SSA and CEC were the lowest (Table 1). As for the isotherm adsorption models, Fidel et al. (2018) found Langmuir and Freundlich models suitable for nitrate sorption, but Chintala et al. (2013) had reported that Freundlich isotherms performed well for nitrate sorption as compared to that of Langmuir isotherms. Similarly, Aghoghovwia et al. (2020) verified the findings of the two models, and showed opposite findings that only linear adsorption isotherm performed well with the biochar adsorption for nitrate at 100 mg L^{-1}. The present study has also confirmed the finding as the adsorption of biochar for nitrate was found well by Freundlich model and linear model compared to Langmuir model.

The adsorption of phosphate by biochar

As given in the Table 1, the biochar in our study might release phosphate into the aqueous solutions due to high phosphate content in biochar itself. The adsorption of phosphate was affected by feedstock, pyrolysis temperature, and phosphate concentration (Figure 4). The minimal phosphate concentration for the adsorption by coconut shell biochar was higher than by banana stem biochar. Meanwhile, the required phosphate concentration for the adsorption by banana stem biochar produced in high pyrolysis temperature was lower than that in low temperature. The results of this study are much closer to the previous study of Luo et al. (2019). Hollister et al. (2013) also obtained the same results on phosphate sorption by using corn straw biochar, but Pratiwi et al. (2016) observed that almost no phosphate sorption was done by the rice husk biochar. Instead, some phosphate ions were released into aqueous solution with lower concentrations below 60 mg P L^{-1}. Zhou et al. (2019) also suggested that biochar derived from plant waste has the limited P adsorption, but adsorption capacity of P can be improved by adjusting pyrolysis temperature. Yin et al. (2018) also had reported that sesame straw biochar derived at 700°C absorbed the optimal phosphate from the solution compared to the sesame biochar derived at the temperature from 300 or 500°C, while Trazzi et al. (2016) also concluded that the adsorption of P on biochar was endothermic and increased with the increase of temperature. Zhao et al. (2017) found that the phosphorus adsorption on biochar increased with the increasing concentration of phosphorus in the solutions, which seemed to be in agreement with the findings of Zhang et al. (2016). The adsorption of phosphate via ligand exchange, cation bridge, and P precipitation involves many other factors including the porous structure, high specific surface area, metal oxide, and surface functional groups (Ghodszad et al. 2021).

Conclusions

Based on the findings obtained in the present study, it can be concluded that the biochar derived from coconut shell or banana stem effectively adsorbed ammonium and nitrate from the aqueous solution. Both Freundlich and Langmuir models were found to fit well ammonium adsorption, while Langmuir model did not perform well for nitrate adsorption. For banana stem biochar, the maximum ammonium adsorption capacity (Q_m) was found in the biochar derived at a low temperature (300°C), but coconut shell biochar derived at a higher temperature (700°C) performed better for ammonium adsorption. The phosphate adsorption by biochars derived by us was not found to be fit by Freundlich and Langmuir models. The minimum phosphate concentration for biochar adsorption decreased with the increasing pyrolysis temperature. Overall, the adsorption of ammonium, nitrate, and phosphate by biochar was related to the feedstock, pyrolysis temperature, and aquatic nutrient concentration. In the future, the comparative study on the mechanism of nitrogen and phosphorus adsorption by various typical biochars should be conducted. Meanwhile, the effect of oxygen-limited method in pyrolysis on the properties of biochar, which would affect the biochar adsorption capacity, is also an interesting work.

Acknowledgments

Authors are thankful to the Hainan Provincial Natural Science Foundation of China (319QN277 & 322RC751), the Central Public-interest Scientific Institution Basal Research Fund for Chinese Academy of Tropical Agricultural Sciences (1630042022010).

References

Aghoghovwia, M.P., Hardie, A.G. & Rozanov, A.B. (2020). Characterisation, adsorption and desorption of ammonium and nitrate of biochar derived from different feedstocks. *Environmental Technology*, 43, pp. 774–787, DOI: 10.1080/09593330.2020.1804466

Bao, S.D. (2000). *Soil agricultural chemical analysis (3rd Edition)*, China Agricultural Press, Beijing 2000.

Carpenter, S.R. (2008). Phosphorus control is critical to mitigating eutrophication. *PANS*, 105, pp. 11039-11040, DOI: 10.1073/pnas.0806112105

Chintala, R., Mollinedo, J., Schumacher, T.E., Papiernik, S.K., Malo, D.D., Clay, D.E., Kumar, S. & Gulbrandson, D.W. (2013). Nitrate sorption and desorption in biochars from fast pyrolysis. *Microporous and Mesoporous Materials*, 179, pp. 250–257, DOI: 10.1016/j.micromeso.2013.05.023

Fidel, R.B., Laird, D.A. & Spokas, K.A. (2018). Sorption of ammonium and nitrate to biochars is electrostatic and pH-dependent. *Scientific Reports*, 8, pp. 1–10, DOI: 10.1038/s41598-018-35534-w

Freundlich, H.M.F. (1907). Über die Adsorption in Lösungen. *Z Phys Chem*, 57, pp. 385–470.

Gai, X., Wang, H., Liu, J., Zhai, L., Liu, S., Ren, T. & Liu, H. (2014). Effects of feedstock and pyrolysis temperature on biochar adsorption of ammonium and nitrate. *PloS One*, 9, pp. e113888. DOI: 10.1371/journal.pone.0113888

Ghodszad, L., Reyhanitabar, A., Maghsoodi, M.R., Lajayer, B.A. & Chang, S.X. (2021). Biochar affects the fate of phosphorus in soil and water: A critical review. *Chemosphere*, 283, pp. 131176, DOI: 10.1016/j.chemosphere.2021.131176

Hale, S.E., Alling, V., Martinsen, V., Mulder, J., Breedveld, G.D. & Cornelissen, G. (2013). The sorption and desorption of phosphate-P, ammonium-N and nitrate-N in cacao shell and corn cob biochars. *Chemosphere*, 91, pp. 1612–1619, DOI: 10.1016/j.chemosphere.2012.12.057

Hu, X., Zhang, X., Ngo, H.H., Guo, W., Wen, H., Li, C., Zhang, Y. & Ma, C. (2020). Comparison study on the ammonium adsorption of the biochars derived from different kinds of fruit peel. *Science of the Total Environment*, 707, pp. 135544, DOI: 10.1016/j.scitotenv.2019.135544

Huang, M., Yang, L., Qin, H., Jiang, L. & Zou, Y. (2014). Fertilizer nitrogen uptake by rice increased by biochar application. *Biology and Fertility of Soils*, 50, pp. 997–1000, DOI: 10.1007/s00374-014-0908-9

Hollister, C.C., Bisogni, J.J. & Lehmann, J. (2013). Ammonium, nitrate, and phosphate sorption to and solute leaching from biochars prepared from corn stover (*Zea mays L.*) and oak wood (*Quercus spp.*). *Journal of Environmental Quality*, 42, pp. 137–144, DOI: 10.2134/jeq2012.0033

Hou, J., Huang, L., Yang, Z., Zhao, Y., Deng, C., Chen, Y. & Li, X. (2016). Adsorption of ammonium on biochar prepared from giant reed. *Environmental Science and Pollution Research*, 23, pp. 19107–19115, DOI: 10.1007/s11356-016-7084-4

Jassal, R.S., Johnson, M.S., Molodovskaya, M., Black, T.A., Jollymore, A. & Sveinson, K. (2015). Nitrogen enrichment potential of biochar in relation to pyrolysis temperature and feedstock quality. *Journal of Environmental Management*, 152, pp. 140–144, DOI: 10.1016/j.jenvman.2015.01.021

Kameyama, K., Miyamoto, T., Iwata, Y. & Shiono, T. (2016). Influences of feedstock and pyrolysis temperature on the nitrate adsorption of biochar. *Soil Science and Plant Nutrition*, 62, pp. 180–184, DOI: 10.1080/00380768.2015.1136553

Kim, J., Yoo, G., Kim, D., Ding, W. & Kang, H. (2017). Combined application of biochar and slow-release fertilizer reduces methane emission but enhances rice yield by different mechanisms. *Applied Soil Ecology*, 117, pp. 57–62, DOI: 10.1016/j.apsoil.2017.05.006

Kong, L.L., Liu, W.T. & Zhou, Q.X. (2014). Biochar: an effective amendment for remediating contaminated soil. *Reviews of Environmental Contamination and Toxicology*, 228, pp. 83–99, DOI: 10.1007/978-3-319-01619-1_4

Langmuir, I. (1916). The constitution and fundamental properties of solids and liquids. Part I. Solids. *Journal of the American Chemical Society*, 38, pp. 2221–2295, DOI: 10.1021/ja02268a002

Laird, D., Fleming, P., Wang, B., Horton, R. & Karlen, D. (2010). Biochar impact on nutrient leaching from a Midwestern agricultural soil. *Geoderma*, 158, pp. 436–442, DOI: 10.1016/j.geoderma.2010.05.012

Lu, C. & Tian, H. (2017). Global nitrogen and phosphorus fertilizer use for agriculture production in the past half century: shifted hot spots and nutrient imbalance. *Earth System Science Data*, 9, pp. 181–192, DOI.org/10.5194/essd-9-181-2017

Luo, L., Wang, G., Shi, G., Zhang, M., Zhang, J., He, J., Xiao, Y., Tian, D., Zhang, Y., Deng, S., Zhou, W., Lan, T. & Deng, O. (2019). The characterization of biochars derived from rice straw and swine manure, and their potential and risk in N and P removal from water. *Journal of Environmental Management*, 245, pp. 1–7, DOI: 10.1016/j.jenvman.2019.05.072

Norman, R.J., Edberg, J.C. & Stucki, J.W. (1985). Determination of nitrate in soil extracts by dual-wavelength ultraviolet spectrophotometry. *Soil Science Society of America Journal*, 49, pp. 1182–1185, DOI: 10.2136/sssaj1985.03615995004900050022x

Piekarski, J., Dąbrowski, T., Dąbrowski, J. & Ignatowicz, K. (2021). Preliminary studies on odor removal in the adsorption process on biochars produced form sewage sludge and beekeeping waste. *Archives of Environmental Protection*, 47, pp. 20–28, DOI: 10.24425/aep.2021.137275

Pratiwi, E.P.A., Hillary, A.K., Fukuda, T. & Shinogi, Y. (2016). The effects of rice husk char on ammonium, nitrate and phosphate retention and leaching in loamy soil. *Geoderma*, 277, pp. 61–68, DOI: 10.1016/j.geoderma.2016.05.006

Pulka, J., Wiśniewski, D., Gołaszewski, J. & Białowiec, A. (2016). Is the biochar produced from sewage sludge a good quality solid fuel. *Archives of Environmental Protection*, 42, pp. 125–134, DOI: 10.1515/aep-2016-0043

Takaya, C.A., Fletcher, L.A., Singh, S., Anyikude, K.U. & Ross, A.B. (2016). Phosphate and ammonium sorption capacity of biochar and hydrochar from different wastes. *Chemosphere*, 145, pp. 518–527, DOI: 10.1016/j.chemosphere.2015.11.052

Tian, H., Lu, C., Melillo, J., Ren, W., Huang, Y., Xu, X., Liu, M., Zhang, C., Chen, G., Pan, S., Liu, J. & Reilly, J. (2012). Food benefit and climate warming potential of nitrogen fertilizer uses in China. *Environmental Research Letters*, 7, pp. 044020, DOI: 10.1088/1748-9326/7/4/044020

Trazzi, P.A., Leahy, J.J., Hayes, M.H. & Kwapinski, W. (2016). Adsorption and desorption of phosphate on biochars. *Journal of Environmental Chemical Engineering*, 4, pp. 37–46, DOI: 10.1016/j.jece.2015.11.005

Vijayaraghavan, K. & Balasubramanian, R. (2021). Application of pinewood waste-derived biochar for the removal of nitrate and phosphate from single and binary solutions. *Chemosphere*, 278, pp. 130361, DOI: 10.1016/j.chemosphere.2021.130361

Xu, D., Cao, J., Li, Y., Howard, A. & Yu, K. (2019). Effect of pyrolysis temperature on characteristics of biochars derived from different feedstocks: A case study on ammonium adsorption capacity. *Waste Management*, 87, pp. 652–660, DOI: 10.1016/j.wasman.2019.02.049

Ye, L., Zhao, X., Bao, E., Li, J., Zou, Z. & Cao, K. (2020). Bio-organic fertilizer with reduced rates of chemical fertilization improves

soil fertility and enhances tomato yield and quality. *Scientific Reports*, 10, pp. 1–11, DOI: 10.1038/s41598-019-56954-2

Yin, H., Zhao, W., Li, T., Cheng, X. & Liu, Q. (2018). Balancing straw returning and chemical fertilizers in China: Role of straw nutrient resources. *Renewable and Sustainable Energy Reviews*, 81, pp. 2695–2702, DOI: 10.1016/j.rser.2017.06.076

Yin, Q., Zhang, B., Wang, R. & Zhao, Z. (2018). Phosphate and ammonium adsorption of sesame straw biochars produced at different pyrolysis temperatures. *Environmental Science and Pollution Research*, 25, pp. 4320–4329, DOI: 10.1007/s11356-017-0778-4

Zhang, H., Chen, C., Gray, E.M., Boyd, S.E., Yang, H. & Zhang, D. (2016). Roles of biochar in improving phosphorus availability in soils: a phosphate adsorbent and a source of available phosphorus. *Geoderma*, 276, pp. 1–6, DOI: 10.1016/j.geoderma.2016.04.020

Zhao, H., Xue, Y., Long, L. & Hu, X. (2018). Adsorption of nitrate onto biochar derived from agricultural residuals. *Water Science and Technology*, 77, pp. 548–554, DOI: 10.2166/wst.2017.568

Zhao, S., Wang, B., Gao, Q., Gao, Y. & Liu, S. (2017). Adsorption of phosphorus by different biochars. *Spectroscopy Letters*, 50, pp. 73–80, DOI: 10.1080/00387010.2017.1287091

Zhou, L., Xu, D., Li, Y., Pan, Q., Wang, J., Xue, L. & Howard, A. (2019). Phosphorus and nitrogen adsorption capacities of biochars derived from feedstocks at different pyrolysis temperatures. *Water*, 11, pp. 1559, DOI: 10.3390/w11081559